International Archives of
Addiction Research and Medicine

Inhibitory Potential of *Struchium sparganophora* Phytochemicals on Cyclooxygenases and Their Health Implications on Inflammations and Pains

Ololade Zacchaeus S[1]*, Oyebanji Olawumi T[1], Onifade Olayinka F[2], Olaniran Anikeola C[1], Idowu Oluwatope O[1], Quadri-Oloye Mariam T[1] and Tommy Bessie E[1]

[1]Department of Chemistry, Medicinal and Organic Chemistry Unit, University of Medical Sciences, Ondo, Nigeria

[2]Department of Chemical and Food Sciences, Biochemistry Unit, Bells University of Technology, Ota, Nigeria

*Corresponding author: *Ololade Zacchaeus S, Department of Chemistry, Medicinal and Organic Chemistry Unit, University of Medical Sciences, Ondo, Nigeria, Tel: +2348034836546*

Abstract

The inhibition of cyclooxygenases provides analgesic effect to relief inflammation and pain. The *in silico* study herein aimed to predict and elucidate the inhibitory potential of *S. Sparganophora* phytochemicals on the enzymes. An integrated molecular modeling approach which includes molecular docking, MMGBA, and pharmacokinetic profiling was employed to identify potential inhibitors of COX-1 and COX-2 from the characterized phytochemicals of *S. Sparganophora*. The results showed that myristic acid (-9.124), palmitic acid (-8.276), xanthinin (-8.063), 2,3-dehydro-4-oxo-beta-ionol (-7.596), coniferyl alcohol (-7.484) and alpha-D-glucopyranoside (-7.406) exhibited good binding to COX-1. Furthermore, alpha-D-glucopyranoside (-8.116), ambrosiol (-7.437), 2,3,5,5,8a-pentamethyl-6,7,8,8a-tetrahydro-5H-chromen-8-ol (-7.392), (7E)-2,6,6-trimethyl-3-methylene-7-(3-oxobutylidene) oxepanyl acetate (-7.392), (8S,14)-cedran-diol (-7.362), and 3-oxo-10(14)-epoxyguai-11(13)-en-6,12-olide (-7.183) ranked highly in binding to COX-2. It is worthy to note that alpha D-glucopyranoside showed robust binding to both protein targets and could be explored as a dual inhibitor of both proteins. Furthermore, pharmacokinetic studies showed that the reported compounds have good prospects of being oral anti-inflammatory drug candidates. These findings suggest that the reported compounds could be explored as inhibitors of COX-1 and COX-2.

Keywords

Struchium sparganophora, Phytochemicals, Cyclooxygenases, Pharmacokinetic, Lipinski rule

Introduction

Vegetables are the most important sources of vitamin A, a nutrient important for several metabolic activities in the body, in addition to its role as antioxidant; vegetables provide folate and potassium that are known to prevent birth defects, cancer, heart disease, hypertension and stroke; vegetables are good sources of phytochemicals [1-5]. A diet rich in vegetables and fruits can lower blood pressure, reduce the risk of heart disease and stroke, prevent some types of cancer, lower risk of eye and digestive problems, and have a positive effect upon blood sugar, which can help keep appetite in check. Most vegetables are naturally low in fat and calories [4,5]. Vegetables are important sources of many nutrients, including potassium, dietary fiber, folate, vitamin A, and vitamin C. Diets rich in potassium may help to maintain healthy blood pressure [5-9]. *Struchium sparganophora*, (Linn.) *Asteraceae* is a culinary herb consumed by Africans and it is known to have a nutritive and medicinal values. The green vegetable plays significant role in human nutrition, especially as a source of vitamins, minerals and dietary fibre. *S. Sparganophora* is a medicinal herb useful in the treatment of pain, fever, arthritis, rheumatism, neurological and mental disorders in traditional system of medicine in Nigeria and some other Africa countries [10,11]. Cyclooxygenase (COX) is an enzyme that helps create the chemicals

prostaglandin and thromboxane (TxA2). Prostaglandins help create inflammation, and TxA2 helps in blood clot [12-15]. Cyclooxygenase (COX) enzymes, COX-1 and COX-2, are responsible for the catalysis of prostaglandin synthesis from its precursor arachidonic acid. COX-2 is normally undetectable in healthy tissue, though increased amounts of COX-2 can be detected in premalignant and in malignant tissue [12,16-18]. Both COX-1 and COX-2 produce the prostaglandins that contribute to pain, fever, and inflammation [12,15,19-21]. Cyclooxygenase metabolites have diverse effects in the lung and are known to modify airway tone, as well as inflammatory responses [15,16,22-25]. To the best of our knowledge, there is paucity information on the chemical composition and inhibitory potential of *S. Sparganophora* phytochemicals on cyclooxygenases so far. Therefore, this study was carried out to investigate and elucidate the inhibitory potential of *S. Sparganophora* phytochemicals on the enzymes (COX-1 and COX-2) to provide analgesic effect to relief inflammation and pain.

Materials and Methods

Ligands and protein targets

To identify potential inhibitors of COX-1 and COX-2, the compounds identified from our GC-MS analysis of *S. Sparganophora* were retrieved from Pub Chem repository in 2D sdf format [26,27]. Subsequently, the crystal structures of COX-1 (PDB ID: 1CQE) and COX-2 (PDB ID: 5KIR) were downloaded from Protein Data Bank (http://www.rscb.org/).

Ligand preparation

The bioactive compounds of *S. Sparganophora* to be screened during the molecular docking were initially prepared using the functional Lig Prep tool in Maestro. In details, the ionization states and tautomers of the compounds were generated at pH = 7.2 ± 0.2 and subsequently optimized using the OPLS 2005 force field [27,28].

Protein preparation and receptor grid generation

To prepare the targets for the molecular docking procedure, the protein structures were initially incorporated into Maestro and then prepared using the Protein Preparation Wizard. Specifically, the missing side chains were added using prime, solvents and other non-standard ligands were removed, hydrogen positions were optimized and restrained energy minimization was performed on the proteins [28]. Furthermore, grid boxes were generated using the position of the co-crystallized ligand of the proteins to map out the binding pockets and subsequently guide the automated docking procedure.

Molecular docking

To identify compounds with potent inhibitory interactions with COX-1 and COX-2, the molecular docking procedure was carried out using the Glide script on maestro 11.1 [29]. The compounds were docked into the binding pockets of the protein targets guided by the prepared grid of the protein targets [30]. The results from the most rigorous screening (XP) were exported for further analysis.

MMGBSA

The binding free energy change calculations were performed using Molecular Mechanics Generalized Born Surface Area (MM/GBSA) calculation [27,31-34]. The docked complexes were minimized by using local optimization feature in Prime wizard of Maestro [35]. The OPLS-2005 force field was employed to determine the binding energy for a set of receptor and ligand.

The binding free energy was estimated using the following equation:

$$\Delta G \text{ bind} = \Delta EMM + \Delta GSolv + \Delta GSA$$

Where, ΔEMM is the variance between the minimized energy of the protein-ligand complexes, while $\Delta GSolv$ is the variation between the GBSA solvation energy of the protein-ligand complexes and the sum of the solvation energies for the protein and ligand. In ΔGSA contains some of the surface area energies in the protein and ligand and the difference in the surface area energies for the complexes. The minimization of the docked complexes was done using a local optimization feature of prime [27,34].

Pharmacokinetic profiling

The ADMET properties of the compounds were predicted using the user-friendly SWISSADME web tool (http://www.swissadme.ch) [36] and the Pro-Tox II web server (https://tox-new.charite.de/protox_II/) [37]. In details, the properties predicted include lipophilicity, water solubility, gastrointestinal absorption, interaction CYP and P-glycoprotein, drug likeness and bioavailability score. Consensus log P, the arithmetic mean of different models of the partition coefficient of n-octanol to water was adopted as the measure of the lipophilicity of the compounds. ESOL model of water solubility (ESOL Log S) was used for solubility and Lipinski rule-based filter was adopted to predict the drug-likeness of the compounds. Furthermore, LD_{50}, carcinogenicity, hepatotoxicity, mutagenicity, cytotoxicity, and immunotoxicity were predicted for the toxicity profiling.
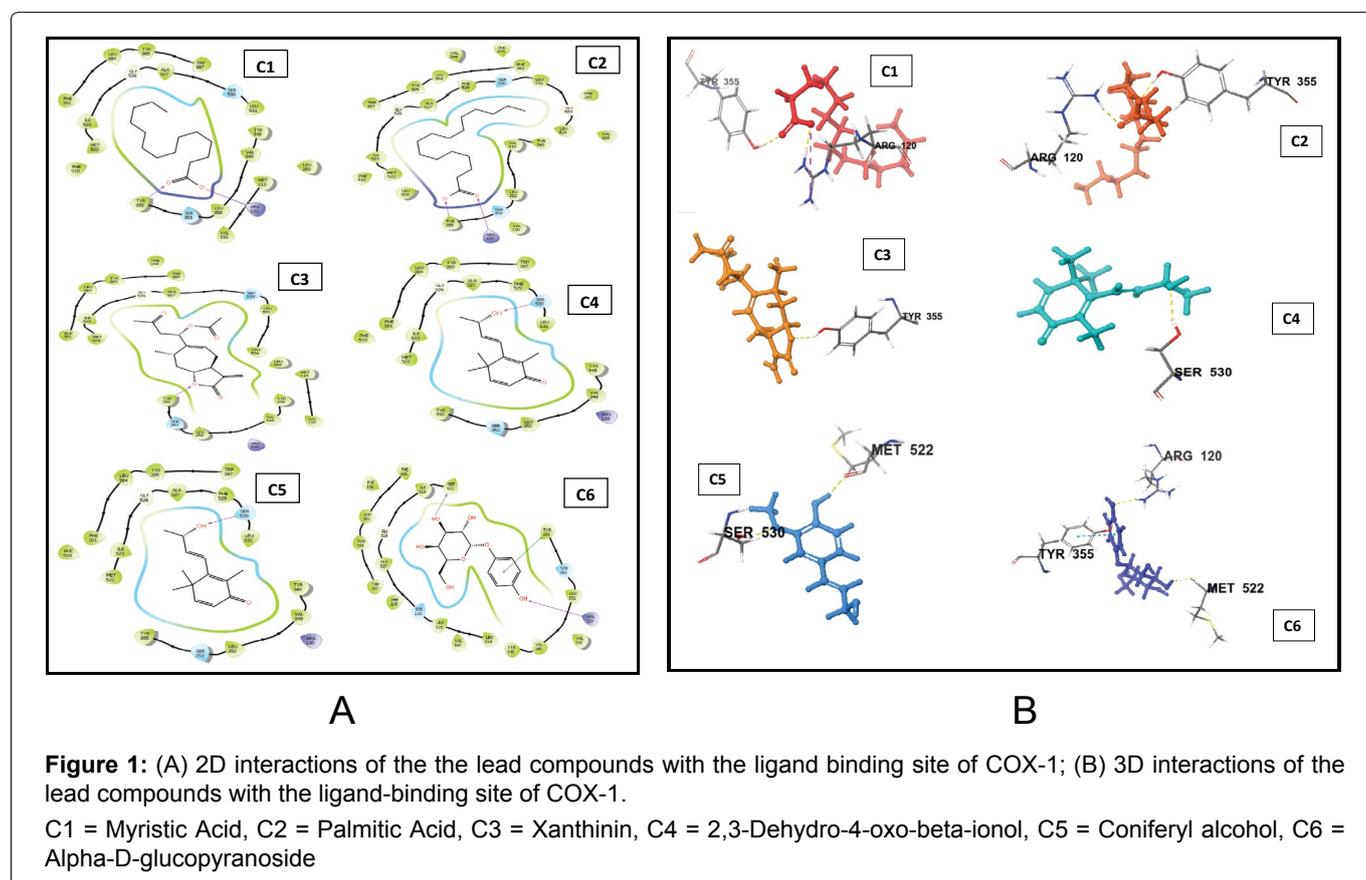
Results and Discussion

The docking scores of the top-scoring compounds against both COX-1 and COX-2 are presented in Table 1. The reported compounds exhibit promising molecular binding to the proteins under study. However, for both protein targets, the standard co-crystallized ligand ranked higher than the test compounds in terms of binding affinity. In details, the standard ligand of COX-

1 had a docking score of -12.212 which is relatively higher than the top scoring test compounds namely myristic acid, palmitic acid, Xanthinin,2,3-Dehydro-4-oxo-beta-ionol, Coniferyl alcohol, and Alpha-D-glucopyranoside which had docking scores of -9.124, -8.276, -8.063, -7.596, -7.484, and -7.406, respectively.

Table 1: Docking scores of the test compounds.

S/N	Compounds	Docking score
	COX-1	
1	myristic acid	-9.124
2	palmitic acid	-8.276
3	Xanthinin	-8.063
4	2,3-Dehydro-4-oxo-beta-ionol	-7.596
5	Coniferyl alcohol	-7.484
6	alpha-D-glucopyranoside	-7.406
7	Co-ligand	-12.212
	COX-2	
1	Alpha-D-glucopyranoside	-8.116
2	Ambrosiol	-7.437
3	2,3,5,5,8a-pentamethyl-6,7,8,8a-tetrahydro-5H-chromen-8-ol	-7.392
4	(7E)-2,6,6-Trimethyl-3-methylene-7-(3-oxobutylidene)oxepanyl acetate	-7.392
5	(8S,14)-cedran-diol	-7.362
6	3-oxo-10(14)-epoxyguai-11(13)-en-6,12-olide	-7.183
7	Co-ligand	-9.72

In similar fashion, the co-crystalizedlig and of COX-2 had a docking score of -9.72 which is relatively higher than alpha-D-glucopyranoside, ambrosiol, 2,3,5,5,8 a-pentamethyl-6,7,8,8a-tetrahydro-5H-chromen-8-ol, (7E)-2,6,6-Trimethyl-3-methylene-7-(3-oxobutylidene) oxepanyl acetate, (8S,14)-cedran-diol, and 3-oxo-10(14)-epoxyguai-11(13)-en-6,12-olide with docking scores of -8.116, -7.437, -7.392, -7.382, -7.352 and -7.173 respectively. Interestingly, the binding affinities of our test compounds to both COX-1 and COX-2 ranked higher than the affinity of the test compounds reported by Omoboyowa on the same targets [38]. The 2D amino acid interaction diagrams (Figure 1 and Figure 2) showed that hydrogen bond is the most prevalent interaction observed in all interactions. It is, however, worthy to note that Alpha D-glucopyranoside exhibited impressive binding to both COX-1 and COX-2 and could be explored as a dual inhibitor of both proteins. The generated poses of the ligands bound to the binding site of the protein targets were re-scored using MMGBSA calculations. This protocol is not new and has shown promising results in identifying small molecule inhibitors of a wide range of proteins. The prime MMGBSA analysis showed the relative binding-free energy (ΔG bind) of each ligand in complex with the ligand-binding site of both target proteins (COX-1 and COX-2), and the results are presented in Figure 3. The trend in the results is similar to that which was obtained from the molecular docking. The standard co-crystallized ligand exhibited the highest binding of all compounds tested against COX-1 with a ΔG value of -55.733 kcal/mol. Myristic acid, palmitic

Figure 1: (A) 2D interactions of the the lead compounds with the ligand binding site of COX-1; (B) 3D interactions of the lead compounds with the ligand-binding site of COX-1.

C1 = Myristic Acid, C2 = Palmitic Acid, C3 = Xanthinin, C4 = 2,3-Dehydro-4-oxo-beta-ionol, C5 = Coniferyl alcohol, C6 = Alpha-D-glucopyranoside
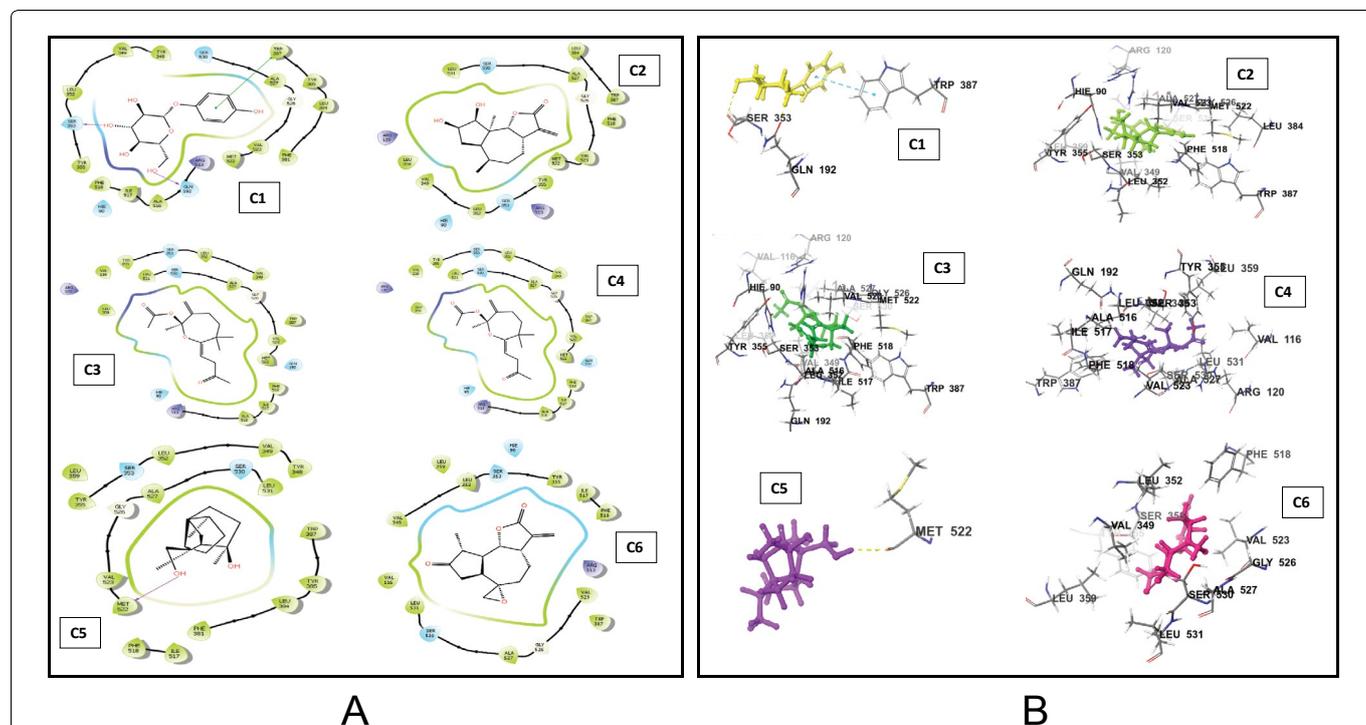
Figure 2: (A) 2D interactions of the lead compounds with the ligand binding site of COX-2; (B) 3D interactions of the lead compounds with the ligand binding site of COX-2.

C1 = Alpha-D-glucopyranoside, C2 = Ambrosiol, C3 = 2,3,5,5,8a-pentamethyl-6,7,8,8a-tetrahydro-5H-chromen-8-ol, C4 = (7E)-2,6,6-Trimethyl-3-methylene-7-(3-oxobutylidene)oxepanyl acetate, C5 = (8S,14)-cedran-diol, C6 = 3-oxo-10(14)-epoxyguai-11(13)-en-6,12-olide.

Figure 3: COX-1: C1 = myristic acid, C2 = palmitic acid, C3 = Xanthinin, C4 = 2,3-Dehydro-4-oxo-beta-ionol, C5 = Coniferyl alcohol, C6 = alpha-D-glucopyranoside

COX-2: C1 = Alpha-D-glucopyranoside, C2 = Ambrosiol, C3 = 2,3,5,5,8a-pentamethyl-6,7,8,8a-tetrahydro-5H-chromen-8-ol, C4 = (7E)-2,6,6-Trimethyl-3-methylene-7-(3-oxobutylidene)oxepanyl acetate, C5 = (8S,14)-cedran-diol, C6 = 3-oxo-10(14)-epoxyguai-11(13)-en-6,12-olide.
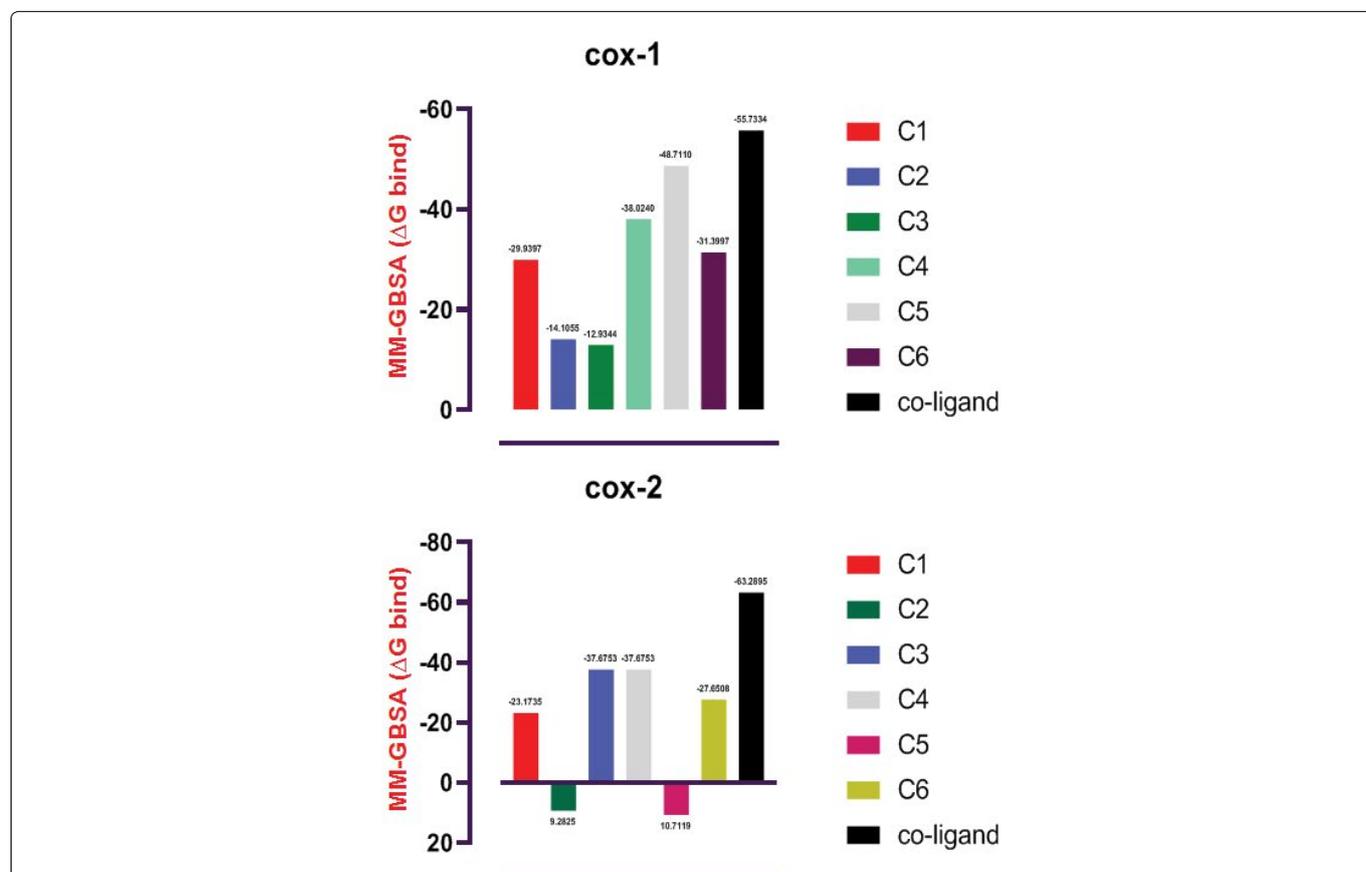
acid, xanthinin, 2,3-Dehydro-4-oxo-beta-ionol, coniferyl alcohol, and alpha-D-glucopyranoside had energy values of -29.940 kcal/mol, -14.106 kcal/mol, -12.934 kcal/mol, -38.024 kcal/mol, -48.711 kcal/mol and -31.340 kcal/mol, respectively. Coniferyl alcohol had the closest binding energy to the co-crystalized ligand. In similar fashion, the co-crystallized ligand of COX-2 also had the highest binding to COX-2 with a ΔG value of -63.290 kcal/mol. Ambrosiol and (8S,14)-cedran-diol showed "positive" ΔG values of 9.282 kcal/mol and 10.712 kcal/mol respectively. 2,3,5,5,8a-pentamethyl-6,7,8,8a-tetrahydro-5H-chromen-8-ol was found to have a similar binding energy to (7E)-2,6,6-Trimethyl-3-methylene-7-(3-oxobutylidene) oxepanyl acetate with a ΔG value of -37.675 kcal/mol. This was observed to be the closest binding energy to the standard co-crystallized ligand. The amino acid interactions of the lead compounds with the ligand binding site of COX-1 and COX-2 were analyzed to identify optimizable ligand-protein interactions. The identification and optimization of the specific interactions can improve the binding affinity of the compounds to their bound receptors. Palmitic acid had two hydrogen bond interactions with the binding pocket of COX-1 (Figure 1) with both bonds occurring as a result of donations from ARG 120 and TYR 355 to the carboxylic group of the compound. Myristic exhibited exactly the same binding conformation as Palmitic acid. Coniferyl alcohol had one hydrogen bond interaction with TYR 355. Similarly, Xanthinin showed only one hydrogen bond interaction with SER 530. Furthermore, alpha-D-glucopyranoside had interactions with three amino acids; a hydrogen bond donation to MET 522, an accepted hydrogen bond from ARG 120 and a pi-stacking between the aromatic ring of the compound and TYR 355, an aromatic amino acid residue. 2,3-Dehydro-4-oxo-beta-ionol had just one interaction with the binding pocket of COX-1; a hydrogen bond

accepted from SER 530. Remarkably, these amino acid interactions have been reported in the inhibition of COX-1 [38]. In its characteristic binding to the ligand-binding site of COX-2, alpha-D-glucopyranoside, the proposed dual inhibitor made contact with three amino acid residues; hydrogen bond donations to SER 353 and GLN 192 and a pi-stacking between the aromatic group of the compound and TRP 387, an aromatic amino acid residue. Also, (8S,14)-cedran-diol exhibited one hydrogen bond interaction with MET 522. However, no hydrogen bond interaction was observed in the binding of ambrosiol, 2,3,5,5,8a-pentamethyl-6,7,8,8a-tetrahydro-5H-chromen-8-ol, (7E)-2,6,6-trimethyl-3-methylene-7-(3-oxobutylidene) oxepanyl acetate, and 3-oxo-10(14)-epoxyguai-11(13)-en-6,12-olide to the pocket of COX-2. More rigorous molecular modeling approach might be required to fully understand and elucidate the specific binding characteristics of these compounds.

Pharmacokinetic profiling

The lipophilicity and water solubility of the lead compounds are presented in Table 2. All the compounds showed good levels of lipophilicity required to have a smooth movement across the intestinal barrier. Palmitic acid was predicted to be the most lipophilic with a log P value of 5.2 and alpha-D-glucopyranoside the least lipophilic with a value of -0.17. A drug candidate must have a sufficient lipophilicity that aids its transport from the gastrointestinal tract into systemic circulation. Complementarily, water solubility facilitates the movement of the drug molecule in the hydrophilic condition of the blood. Drugs are transported to their sites of action through the blood by binding to resident transport molecules in the blood such as albumin. As per ESOL model of water solubility, alpha-D-glucopyranoside showed the highest level of water solubility with a value

Table 2: The physicochemical properties of the lead compounds.

Compounds	Molecular weight	Consensus Log P	ESOL Log S
C1	228.37	4.45	-4.31
C2	256.4	5.2	-5.02
C3	306.35	2.2	-2.28
C4	206.28	2.32	-2.28
C5	180.2	1.62	-2.23
C6	272.25	-0.77	-0.71
C7	266.33	1.71	-2.68
C8	280.36	2.96	-2.78
C9	280.36	2.96	-2.78
C10	238.37	2.69	-2.93
C11	262.3	1.77	-2.19

C1 = Myristic Acid, C2 = Palmitic Acid, C3 = Xanthinin, C4 = 2,3-Dehydro-4-oxo-beta-ionol, C5 = Coniferyl alcohol, C6 = alpha-D-glucopyranoside, C7 = Ambrosiol, C8 = 2,3,5,5,8a-pentamethyl-6,7,8,8a-tetrahydro-5H-chromen-8-ol, C9 = (7E)-2,6,6-Trimethyl-3-methylene-7-(3-oxobutylidene) oxepanyl acetate, C10 = (8S,14)-cedran-diol, C11 = 3-oxo-10(14)-epoxyguai-11(13)-en-6,12-olide

Table 3: The pharmacokinetic profiles of the top-scoring compounds.

	GI Absorption	Pgp substrate	CYP1A2 inhibitor	CYP2C19 inhibitor	CYP2C9 inhibitor	CYP2D6 inhibitor	CYP3A4 inhibitor
C1	High	No	Yes	No	No	No	No
C2	High	No	Yes	No	Yes	No	No
C3	High	No	No	No	No	No	No
C4	High	No	No	No	No	No	No
C5	High	No	No	No	No	No	No
C6	High	No	No	No	No	No	No
C7	High	No	No	No	No	No	No
C8	High	No	No	Yes	No	No	No
C9	High	No	No	Yes	No	No	No
C10	High	No	No	No	No	No	No
C11	High	No	No	No	No	No	No

C1 = Myristic Acid, C2 = Palmitic Acid, C3 = Xanthinin, C4 = 2,3-Dehydro-4-oxo-beta-ionol, C5 = Coniferyl alcohol, C6 = alpha-D-glucopyranoside, C7 = Ambrosiol, C8 = 2,3,5,5,8a-pentamethyl-6,7,8,8a-tetrahydro-5H-chromen-8-ol, C9 = (7E)-2,6,6-Trimethyl-3-methylene-7-(3-oxobutylidene) oxepanyl acetate, C10 = (8S,14)-cedran-diol, C11 = 3-oxo-10(14)-epoxyguai-11(13)-en-6,12-olide

Table 4: The druglikeness and bioavailability score of the test compounds.

Compounds	Lipinski # violations	Bioavailability Score
C1	0	0.85
C2	1	0.85
C3	0	0.55
C4	0	0.55
C5	0	0.55
C6	0	0.55
C7	0	0.55
C8	0	0.55
C9	0	0.55
C10	0	0.55
C11	0	0.55

C1 = Myristic Acid, C2 = Palmitic Acid, C3 = Xanthinin, C4 = 2,3-Dehydro-4-oxo-beta-ionol, C5 = Coniferyl alcohol, C6 = alpha-D-glucopyranoside, C7 = Ambrosiol, C8 = 2,3,5,5,8a-pentamethyl-6,7,8,8a-tetrahydro-5H-chromen-8-ol, C9 = (7E)-2,6,6-Trimethyl-3-methylene-7-(3-oxobutylidene) oxepanyl acetate, C10 = (8S,14)-cedran-diol, C11 = 3-oxo-10(14)-epoxyguai-11(13)-en-6,12-olide

of -0.71 and palmitic, the least soluble with an ESOL Log S value of -5.02.

The pharmacokinetic profiles of the top-scoring compounds are presented in Table 3. All compounds have a high gastrointestinal absorption. Oral drug candidates must have a structural orientation which enables them cross the lumen of the small intestine into systemic circulation. A high gastrointestinal absorption results from a good lipophilicity-hydrophilicity ratio. Also, none of the compounds is predicted to be a substrate of permeability glycoprotein. This protein is a member of the ATP-binding cassette proteins which orchestrates the active transport of compounds out of the cell before reaching a significant therapeutic concentration in the cell. Xanthinin, 2,3-Dehydro-4-oxo-beta-ionol, Coniferyl alcohol, alpha-D-glucopyranoside, Ambrosiol, (8S,14)-cedran-diol, and 3-oxo-10(14)-epoxyguai-11(13)-en-6,12-olide are non-inhibitors of the vital CYP isoforms. This family of enzymes catalyze phase 1 reaction of drug metabolism which contributes substantially to the clearance of the compounds. Inhibiting any of the participating isoforms can induce a drug-drug interaction which elicits the toxic effects of the drug due to its delayed clearance.

The drug likeness and bioavailability score of the top-scoring compounds are presented in Table 4. These complementary properties predict the oral drug candidacy of small molecular weight compounds. The result showed that palmitic acid violated one of the Lipinski rule-of-five where all the other compounds violated none of the rules. The Lipinski rule of five for drug-likeness showed that all the compounds are drug-like. The rule is valid when mol. MW < 500, QPlogPo/w < 5, donor HB ≤ 5, acceptor HB ≤ 10 [39]. This rule-based filter is constantly employed in drug design to predict the likelihood of a compound being an oral drug candidate. Furthermore, all the reported compounds had positive bioavailability scores. Myristic acid and palmitic acid had a bioavailability score of 0.85 while the other compounds returned a bioavailability score of 0.55. In general, a bioavailability score of at least 0.10 is required to be considered a candidate [40].

The toxicity profiles of the compounds are presented in Table 5. Generally, Pro Tox-II presents the mutagenicity, carcinogenicity, immunotoxicity, hepatotoxicity, and cytoxicity profiles of chemical compounds. Additionally, it places chemical compounds into 6

Ololade et al. Int Arch Addict Res Med 2024, 9:039

• Page 6 of 8 •

Table 5: The toxicity profiles of the lead compounds.

Compounds	LD_{50} (mg/kg)	TC	CG	HT	MG	CT	IT	PA
C1	900	4	-	-	-	-	-	100
C2	900	4	-	-	-	-	-	100
C3	1320	4	-	-	-	-	+	69.26
C4	2000	4	-	-	-	-	-	68.07
C5	2500	5	-	-	-	-	+	70.97
C6	23000	6	-	-	-	-	-	67.38
C7	150	3	-	-	-	-	+	69.26
C8	6060	6	-	-	-	-	-	67.38
C9	2000	4	-	-	-	-	-	68.07
C10	2000	4	-	-	-	-	-	70.97
C11	150	3	-	-	-	-	+	69.26

C1 = Myristic Acid, C2 = Palmitic Acid, C3 = Xanthinin, C4 = 2,3-Dehydro-4-oxo-beta-ionol, C5 = Coniferyl alcohol, C6 = alpha-D-glucopyranoside, C7 = Ambrosiol, C8 = 2,3,5,5,8a-pentamethyl-6,7,8,8a-tetrahydro-5H-chromen-8-ol, C9 = (7E)-2,6,6-Trimethyl-3-methylene-7-(3-oxobutylidene) oxepanyl acetate, C10 = (8S,14)-cedran-diol, C11 = 3-oxo-10(14)-epoxyguai-11(13)-en-6,12-olide.

Key: TC: Toxicity class; CG: Carcinogenicity; HT: Hepatotoxicity; MG: Mutagenicity; CT: Cytotoxicity; IT: Immunotoxicity; PA: Prediction accuracy (%)

classes of toxicity, with Class 1 being the most toxic and Class 6 being the least toxic. Interestingly, all the lead compounds are generally less toxic with LD_{50} (mg/kg) ranging from 900 to 23,000 and toxicity class between 4 to 6, except C7 and C11 with LD_{50} of 150 mg/kg and toxicity class 3. However, none of the compounds is found to be carcinogenic, hepatotoxic, mutagenic or cytotoxic, though C3, C5, C7, and C11 are predicted to be immunotoxic.

Conclusion

The investigated phytochemicals in *S. Sparganophora* exhibit promising pharmacological potential to inhibit COX-1 and COX-2. The binding affinities of our test compounds to both COX-1 and COX-2 ranked higher. All compounds have a high gastrointestinal absorption. The result showed that almost all the compounds violated none of the Lipinski rules. None of the compounds is found to be carcinogenic, hepatotoxic, mutagenic or cytotoxic. Pharmacokinetic studies showed that the reported compounds have good prospects of being oral anti-inflammatory drug candidates. These findings suggest that the reported compounds could be explored as inhibitors of COX-1 and COX-2.

Conflict of Interest

We have no conflict of interest.

Data Availability Statement

The authors confirm that the data supporting the findings of this study are available within the article.

References

1. Rana N, Ghabru A, Vaidya D (2019) Defensive function of fruits and vegetables. Journal of Pharmacognosy and Phytochemistry 8: 1872-1877.

2. Wallace TC, Bailey RL, Blumberg JB, Burton-Freeman B, Oliver Chen C-y, et al. (2020) Fruits, vegetables, and health: A comprehensive narrative, umbrella review of the science and recommendations for enhanced public policy to improve intake. Critical Reviews in Food Science and Nutrition 60: 2174-2211.

3. Mungofa N, Sibanyoni JJ, Mashau ME, Beswa D (2022) Prospective role of indigenous leafy vegetables as functional food ingredients. Molecules 27: 7995.

4. Ololade ZS, Anuoluwa IA, Adeyemi AF, Uyaboerigha DI (2021) Synergistic efficacy of phytochemical, antioxidant and bactericidal properties of the aerial essential oil of laggera crispate. Pharmacognosy Journal 13: 1304-1311.

5. Kibr G (2022) The health benefits of vegetables; preventive implications for chronic non-communicable diseases. Vegetable Crops-Health Benefits and Cultivation.

6. Boeing H, Bechthold A, Bub A, Ellinger S, Haller D, et al. (2012) Critical review: Vegetables and fruit in the prevention of chronic diseases. Eur J Nutr 51: 637-663.

7. Ololade ZS, Olawore NO (2021) Health benefits of the fruit essential oil of eucalyptus citriodora: Secondary metabolites, radical scavenging, antioxidant, antiinflamatory, analgesic, antimicrobial potential. International Journal of Drug Development and Research 13: 1-7.

8. Adesina AR, Ogunmoyela OAB, Arisa NU, Ololade ZS (2022) Optimization of the production of local cheese from cow milk processed with the seed of Moringaoleifera. Journal of Food Processing and Preservation 46: e16189.

9. Usman AM, Sahura RG (2023) Prevalence of intestinal parasites on fruits and vegetables sold in biu local government area of borno state, Nigeria. Dutse Journal of Pure and Applied Sciences 9: 146-152.

10. Saka KL, Kudirat O, James OO, Olugbenga FT (2013) The effects of the leaf water extract of Struchium sparganophora (Linn.) Ktzeasteraceae on the hematopoietic parameters and the organ system of rats. Pak J Pharm Sci 26: 1203-1207.

11. Aderibige AO, Agboola OI, Eduviere AT (2015) Anti-inflammatory and analgesic properties of Struchium

Ololade et al. Int Arch Addict Res Med 2024, 9:039

• Page 7 of 8 •

sparganophora linn leaves in mice. Afr J Med Med Sci 44: 71-77.

12. Lee IT, Yang CM (2013) Inflammatory signalings involved in airway and pulmonary diseases. Mediators Inflamm 2013: 791231.

13. Averett C, Arora S, Zubair H, Singh S, Bhardwaj A, et al. (2014) Molecular targets of Honokiol: A promising phytochemical for effective cancer management. Enzymes 36: 175-193.

14. Bindu S, Mazumder S, Bandyopadhyay U (2020) Non-steroidal anti-inflammatory drugs (NSAIDs) and organ damage: A current perspective. Biochem Pharmacol 180: 114147.

15. Juillion P (2020) What is COX-1 and COX-2? Studybuff.com

16. Gye YP, John WC (2006) Involvement of cyclooxygenase-2 and prostaglandins in the molecular pathogenesis of inflammatory lung diseases. Am J Physiol Lung Cell Mol Physiol 290: L797-L805.

17. Ricciotti E, FitzGerald GA (2011) Prostaglandins and inflammation. Arterioscler Thromb Vasc Biol 31: 986-1000.

18. Desai SJ, Prickril B, Rasooly A (2018) Mechanisms of phytonutrient modulation of cyclooxygenase-2 (COX-2) and inflammation related to cancer. Nutr Cancer 70: 350-375.

19. Rouzer CA, Marnett LJ (2009) Cyclooxygenases: Structural and functional insights. J Lipid Res 50: S29-S34.

20. Zidar N, Odar K, Glavac D, Jerse M, Zupanc T, et al. (2009) Cyclooxygenase in normal human tissues--is COX-1 really a constitutive isoform, and COX-2 an inducible isoform? J Cell Mol Med 13: 3753-3763.

21. Wang B, Wu L, Chen J, Dong L, Chen C, et al. (2021) Metabolism pathways of arachidonic acids: Mechanisms and potential therapeutic targets. Sig Transduct Target Ther 6: 94.

22. Smith CJ, Zhang Y, Koboldt CM, Muhammad J, Zweifel BS, et al. (1998) Pharmacological analysis of cyclooxygenase-1 in inflammation. Proc Natl Acad Sci USA 95: 13313-13318.

23. Hla T, Bishop-Bailey D, Liu CH, Schaefers HJ, Trifan OC (1999) Cyclooxygenase-1 and -2 isoenzymes. Int J Biochem Cell Biol 31: 551-557.

24. Fitzpatrick FA (2004) Cyclooxygenase enzymes: Regulation and function. Curr Pharm Des 10: 577-588.

25. Pannunzio A, Coluccia M (2018) Cyclooxygenase-1 (COX-1) and COX-1 inhibitors in cancer: A review of oncology and medicinal chemistry literature. Pharmaceuticals 11: 101.

26. Kim S, Chen J, Cheng T, Gindulyte A, He J, et al. (2021) PubChem in 2021: New data content and improved web interfaces. Nucleic Acids Research 49: D1388-D1395.

27. Rao P, Patel R, Shukla A, Parmar P, Rawal RM, et al. (2021) Identifying structural-functional analogue of GRL0617, the only well-established inhibitor for papain-like protease (PLpro) of SARS-CoV2 from the pool of fungal metabolites using docking and molecular dynamics simulation. Molecular Diversity 26: 309-329.

28. (2017) Schrodinger release.

29. Friesner RA, Banks JL, Murphy RB, Halgren TA, Klicic JJ, et al. (2004) Glide: A new approach for rapid, accurate docking and scoring. 1. Method and assessment of docking accuracy. J Med Chem 47: 1739-1749.

30. Halgren TA (2009) Identifying and characterizing binding sites and assessing druggability. J Chem Inf Model 49: 377-389.

31. Wang W, Donini O, Reyes CM, Kollman PA (2001) Biomolecular simulations: Recent developments in force fields, simulations of enzyme catalysis, protein-ligand, protein-protein, and protein-nucleic acid noncovalent interactions. Annu Rev Biophys Biomol Struct 30: 211-243.

32. Wang J, Hou T, Xu X (2006) Recent advances in free energy calculations with a combination of molecular mechanics and continuum models. Curr Comput Aided Drug Des 2: 287-306.

33. Kollman PA, Massova I, Reyes C, Kuhn B, Huo S, et al. (2000) Calculating structures and free energies of complex molecules: Combining molecular mechanics and continuum models. Acc Chem Res 33: 889-897.

34. Akinnusi PA, Olubode SO, Alade AA, Ashimi AA, Onawola OL, et al. (2023) Potential inhibitory biomolecular interactions of natural compounds with different molecular targets of diabetes. Bioinformatics and Biology Insights.

35. (2018) Schrödinger release.

36. Daina A, Michielin O, Zoete V (2017) Swiss ADME: A free web tool to evaluate pharmacokinetics, drug-likeness and medicinal chemistry friendliness of small molecules. Sci Rep 2017 3: 42717.

37. Banerjee P, Eckert AO, Schrey AK, Preissner R (2018) ProTox-II: A webserver for the prediction of toxicity of chemicals. Nucleic Acids Res 46: W257-W263.

38. Omoboyowa DA (2021) Sterols from Jatrophatanjorensis leaves exhibit anti-inflammatory potential: In vitro and in silico studies. Bulletin of the National Research Centre 45: 194.

39. Lipinski CA (2004) Lead-and drug-like compounds: the rule-of-five revolution. Drug Discov Today Technol 1: 337-341.

40. Martin YC (2005) A bioavailability score. J Med Chem 48: 3164-3170.